Abnormal blood vessel development and lethality in embryos lacking a single VEGF allele

Peter Carmeliet*, Valérie Ferreira*, Georg Breier†, Saskia Pollefeyt*, Lena Kieckens*, Marina Gertsenstein‡, Michaela Fahrig†, Ann Vandenhoeck*, Kendraprasad Harpal‡, Carmen Eberhardt†, Cath6rine Deciercq*, Judy Pawling‡, Lieve Moons*, Désiré Collen*, Werner Risau† & Andras Nagy‡§

* Center for Transgene Technology and Gene Therapy, Flanders Interuniversity Institute for Biotechnology, KU Leuven, B-3000 Leuven, Belgium
† Max-Planck-Institute for physiologische und Klinische Forschung, W. G. Kerckhoff-Institut, Abteilung Molekulare Zellbiologie, Bad Nauheim, Germany
‡ Samuel Lunenfeld Research Institute, Mount Sinai Hospital, Toronto, Ontario, Canada
§ Department of Medical Genetics, University of Toronto, Ontario, Canada

THE endothelial cell-specific vascular endothelial growth factor (VEGF)[1-5] and its cellular receptors Flt-1 (refs 6,7) and Flk-1 (refs 8,9) have been implicated in the formation of the embryonic vasculature. This is suggested by their colocalized expression during embryogenesis[10,11] and the impaired vessel formation in Flk-1 (ref. 12) and Flt-1 (ref, 13) deficient embryos. However, because Flt-1 also binds placental growth factor[14,15], a VEGF homologue, the precise role of VEGF was unknown. Here we report that formation of blood vessels was abnormal, but not abolished, in heterozygous VEGF-deficient ($VEGF^{+/-}$) embryos, generated by aggregation of embryonic stem (ES) cells with tetraploid embryos (T-ES)[16,17], and even more impaired in homozygous VEGF-deficient ($VEGF^{-/-}$) T-ES embryos, resulting in death at mid-gestation. Similar phenotypes were observed in F_1-$VEGF^{+/-}$ embryos, generated by germline transmission. We believe that this heterozygous lethal phenotype, which differs from the homozygous lethality in VEGF-receptor-deficient embryos, is unprecedented for a targeted autosomal gene inactivation, and is indicative of a tight dose-dependent regulation of embryonic vessel development by VEGF.

Targeted inactivation of one ($VEGF^{+/-}$) or both ($VEGF^{-/-}$) alleles in ES cells was accomplished by replacement of the third common VEGF exon with the gene encoding neomycin phosphotransferase (neo), which caused a frameshift in the VEGF coding sequence[18] (unpublished observations), and deleted six of the eight essential cysteine residues[19,20] (Fig. la, b). Absence of exon 3 was confirmed by reverse transcription-polymerase chain reaction (RT-PCR) (Fig. 1c). Northern blot (Fig. ld-g) and RT-PCR analysis (see Supplementary Information) revealed the presence of two aberrant VEGF transcripts at very low abundance (< 3% of wild type) in $VEGF^{-/-}$ embryos and ES cells, differentiated to cystic embryoid bodies (CEBs), which resulted from splicing into (mRNA-1) or around neo (mRNA-2) and contained a stop codon after 49 residues in neo (mRNA-1) or after 24 out-of-frame residues in VEGF exon 4 (mRNA-2) (Fig. la and see Supplementary Information). These mutant transcripts were similarly detected in $VEGF^{+/-}$ and in $riVEGF^{+/+}$ (containing a randomly integrated targeting vector) CEBs and embryos, and resulted from residual transcription of the randomly integrated targeting vector. Transient transfection of mRNA-2 (Fig. la) in COS cells under the control of the cytornegalovirus promoter did not reveal detectable expression of a mutant VEGF peptide, nor dominant-negative inhibition by such peptide on the expression level of wildtype

VEGF in co-transfection experiments, as evaluated by western blot analysis, metabolic labelling, immunoprecipitation (for data, see Supplementary Information) and by induction of procoagulant activity (not shown), indicating that expression of mRNA-2 does not interfere with wild-type VEGF expression.

To distinguish between tetraploid-derived and targeted ES cell-derived embryonic cells, ROSA-26 embryos[21], which ubiquitously express lacZ, were used as donors for the tetraploid embryos. The marker confirmed that tetraploid. cells were confined to the endoderm of the yolk sac and trophoblast cells in all cases studied (see LacZ-positive cells in the yolk sac in Fig. 2d, e). riVEGF$^{+/+}$, VEGF$^{+/-}$ and VEGF$^{-/-}$ T-ES-cell-derived embryos appeared macroscopically normal at 8.5 days postcoitum (d.p.c.), whereas most of the VEGF$^{+/-}$ and VEGF$^{-/-}$ T-ES-cell-derived embryos were retarded at 9.5 d.p.c. and appeared dead at 10.5 d.p.c. At 8.5 and 9.5 d.p.c., the dorsal aorta was completely normal in the anterior (Fig. 2a) and posterior (not shown) part of riVEGF$^{-/-}$ TES-cell-derived embryos, but was only poorly developed in the VEGF$^{+/-}$ T-ES-cell-derived embryos, where endothelial cells lined a much smaller lumen than normal, especially in the anterior part of the embryo (Fig. 2b, c). At 8.5 d.p.c., the dorsal aorta was missing over its entire length in VEGF$^{-/-}$ T-ES-cell-derived embryos (Fig. 2e). At 9.5 d.p.c., abnormally enlarged vascular structures, lined by endothelial cells and filled with nucleated blood cells, were observed throughout the anterior part of the necrotic embryo instead of the normal dorsal aorta and other blood vessels in VEGF$^{-/-}$ T-ES-cell-derived embryos (Fig. 2f). In the caudal part of the embryo, the dorsal aorta was significantly smaller (not shown). A higher degree of tissue necrosis was observed in the VEGF$^{-/-}$ than in VEGF$^{+/-}$ T-ES cell-derived embryos. RT-PCR analysis for the endothelial cellspecific markers Flt-1, Flk-1 and Tie-2 (also known as Tek) (see Supplementary Information), and in situ hybridization for FIt-1 and Flk-l, and immunostaining for Flk-1 and PECAM/CD31 (not shown) at 8.5 and 9.5 d.p.c. revealed fewer and frequently isolated, disorganized and scattered Flk-1and Flt-1 -expressing cells throughout the VEGF$^{-/-}$ embryo at 8.5 d.p.c., and relatively low amounts of Flt-1 and Tie-2 message (which appear later during development) in VEGF$^{-/-}$ embryos at 9.5 d.p.c., suggesting delayed but not aborted endothelial cell development. Thus, at both 8.5 and 9.5 d.p.c., the VEGF$^{-/-}$ genotype resulted in a more severe phenotype than did the VEGF'$^{+/-}$ genotype.

No viable F_1 VEGF$^{+/-}$ offspring were obtained at birth, indicating embryonic lethality. F_1 VEGF$^{+/-}$ and F_1 VEGF'$^{+/-}$: tie-1-1acZ$^{+/-}$ embryos, in which the endothelial cells express lacZ (owing to its targeting to the endothelial cell-specific tie-1 locus[22]), displayed macroscopic and microscopic abnormalities in embryonic development and vascular growth identical to those of the VEGF$^{+/-}$ T-ES cell-derived embryos (Fig. 2g-1). Quantitative morphometric analysis revealed that fewer endothelial cells lined the smaller lumen of the dorsal aorta in the anterior part of F_1 VEGF'$^{+/-}$ than F_1 VEGF$^{+/+}$ embryos (Table 1a). Immature development and defective interconnections of the embryonic vasculature in F_1 VEGF$^{+/-}$ embryos was confirmed by LacZ staining of whole-mount F_1 VEGF'$^{+/-}$:tie-1-1acZ$^{+/-}$ embryos, which revealed a decreased density of sprouting intersomitic and head mesenchyme vessels (Fig. 3a, b), and by injection of ink in the heart, which made visible the dorsal aorta and head vessels in VEGF$^{+/+}$ T-ES cell-derived embryos but revealed no connection between the heart and the vessel system in VEGF$^{+/-}$ T-ES cell-derived embryos (Fig. 3c, d).

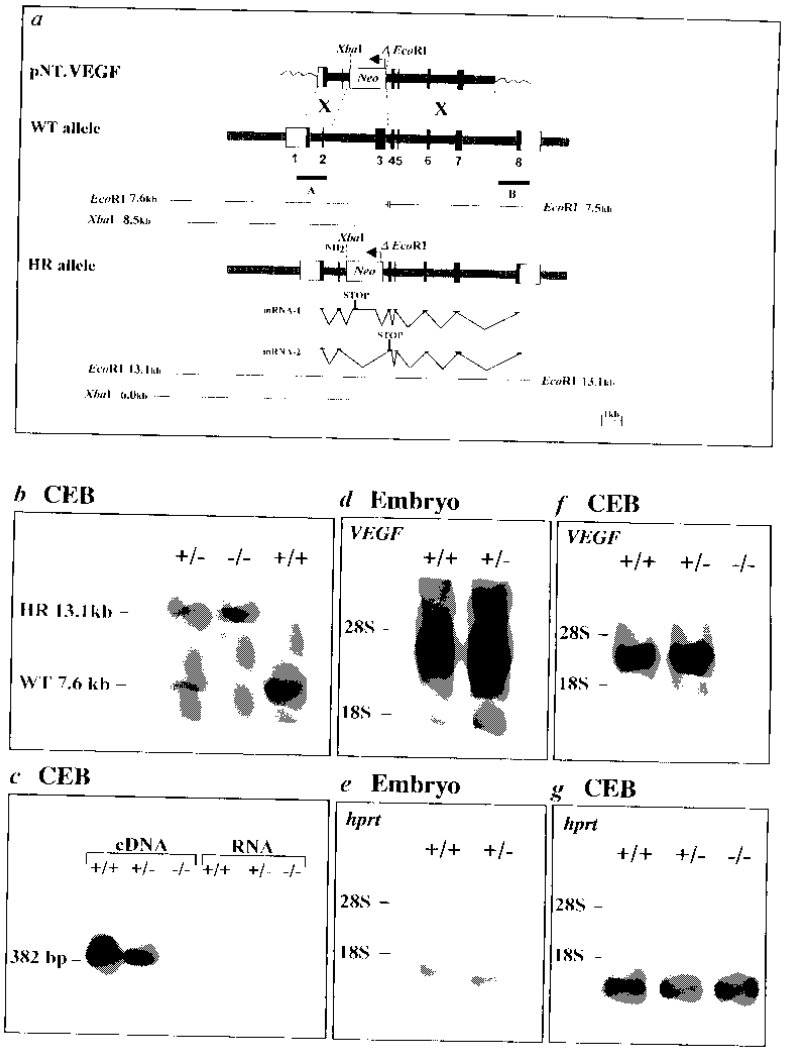

FIG. 1 a, Schematic representation of the targeting vector pNT.VEGF, the wild-type (WT) VEGF allele, and the homologiously recombined (HR) VEGF allele. A 1.8-kb NotI-BamHI fragment and a 5.7-kb EcoRI-NcoI fragment of the murine VEGF gene were cloned into pPNT[25], which destroyed the EcoRI site (ΔEcoRI). mRNA-1 resulted from cryptic splicing from the VEGF exon 2 splice donor site to a splice acceptor site on the non-coding strand of neo (nucleotide 1,373 in pPNT[25]), followed by splicing from a donor sequence in neo, (nucleotide 874 in pPNT[25]) to the splice acceptor site of exon 4. mRNA-2 resulted from splicing from VEGF exon 2, around neo, to exon 4. Shaded boxes represent introns; open boxes, 5' and 3' untranslated regions; filled boxes, coding regions; and closed boxes beneath the gene, hybridization probes. b, Southern blot analysis of genomic DNA, digested with EcoRI and hybridized to probe A, revealing the 7.6-kb and 13.1-kb EcoRI fragment of the WT and HR VEGF alleles, respectively. c, Southern blot analysis of RT-PCR products, using exon 3 and exon 8 primers for amplification and an exon 4 primer for hybridization, revealing allele dosage-dependent reduction of the expected 382bp transcript in $VEGF^{+/-}$ CEBs and absence in $VEGF^{-/-}$ CEBs. Non-transcribed RNA was used as negative control. d-g, Northern blot analysis using a VEGF or hprt probe, revealing a predominant 3.8-kb mRNA in $VEGF^{+/+}$ and $VEGF^{+/-}$ embryos and CEBs, and a 4.1-kb mRNA in $VEGF^{-/-}$ CEBs which represents mRNA-1, as described in a.

METHODS. Four different ES cell lines (D_3, JH_1, RW_4 and R_1) were used for electroporation. Culture and analysis of singly and doubly targeted ES cells were as previously described [26,27]. RT-PCR was done as previously described[28], using oligomers VEGFD in exon 3 (5'-GCCCTGGAGTGCGTGCCCACGTCAGAGAGCA-3') and VEGF8 in exon 8 (5'-GAATTCACCGCCTCGGCTrGTCCACT-3') for amplification and oligomer VEGF11 in exon 4 (5'-CTGGCTTTGGTGAGGMGATCCGCATG-3') for hybridization.

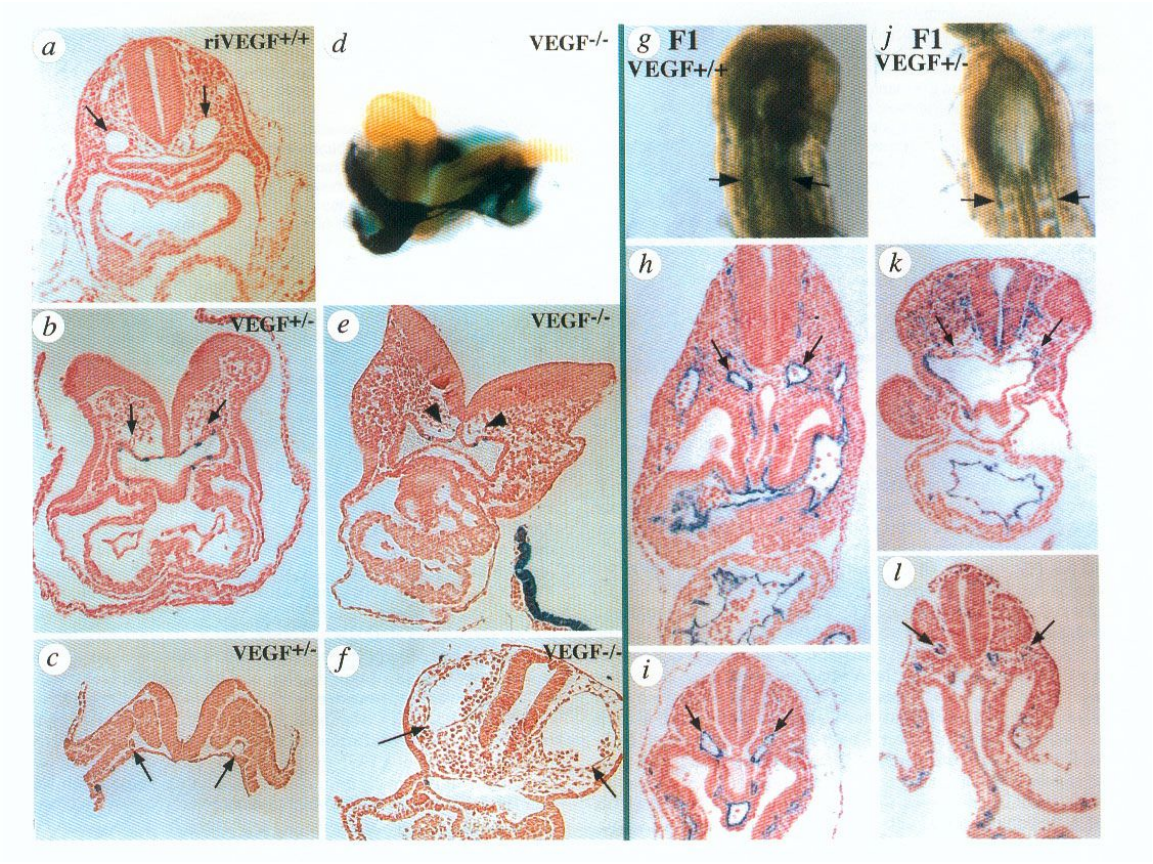

FIG. 2 Vascular development in T-ES cell-derived (a-f) and F_1 VEGF embryos (g-1). a, Normal vascular development in the anterior part of an 8.5-d.p.c. riVEGF$^{+/+}$ T-ES cell-derived embryo. b, c, Reduced diameter of the dorsal aorta (arrows) in the anterior (b) and the posterior (c) part of an 8.5-d.p.c. VEGF$^{+/-}$ embryo. d, LacZ staining of a whole-mount 8.5-d.p.c. VEGF$^{-/-}$ embryo, revealing the yolk sac (blue, tetraploid embryo-derived) and the unstained embryo proper (ES-cell-derived). e, Absence of the dorsal aorta in the anterior part of an 8.5-d.p.c. VEGF$^{-/-}$ embryo. Arrowheads indicate where the dorsal aorta normally develops. f, Abnormally enlarged vascular structures (arrows in f) and significant tissue necrosis in the anterior part of a 9.5-d.p.c. VEGF$^{-/-}$ embryo. g, j, Whole-mount LacZ staining of the posterior part of a 9.5-d.p.c. F_1 VEGF$^{+/+}$: tie-1-1acZ$^{+/-}$ (g), revealing a normal dorsal aorta and of a 9.5-d.p.c. F_1 VEGF$^{+/-}$: tie-1-lacZ$^{+/-}$ (j) embryo, revealing the smaller diameter of the dorsal aorta (arrows point to the dorsal aorta). h, i, Normal dorsal aorta development in both the anterior (h) and posterior (i) part of a 9.5-d.p.c. wild-type embryo. k, 1, The dorsal aorta in the 9.5-d.p.c. F_1 VEGF'$^{+/-}$: tie-l-lacZ$^{+/-}$ embryo was poorly developed in the anterior part, where only a few blue cells formed a string-like aorta (k), and somewhat better in the posterior part, where the dorsal aorta contained a small lumen (1).

METHODS. Completely ES cell-derived embryos were made by aggregation with tetraploid embryos[16,17], using riVEGF$^{+/+}$ and VEGF$^{+/-}$ clones and three daughter VEGF$^{+/-}$ clones that survived the high G418 selection without disruption of the second VEGF-allele and four daughter VEGF$^{-/-}$ clones. No phenotypic differences were observed between embryos obtained from these VEGF$^{+/-}$ clones. VEGF:tie-1-lacZ embryos were genotyped by PCR on yolk sac-derived DNA, using primers VEGFD and VEGF8 (see Fig. 1 legend), and neo-specific primers neoA (5'-AT-TGAACAAGATGGATTGCAC-3', sense direction) and neoB (5'-TTCGTCCAGATCATCCTGATCGAC-3', antisense direction). Embryos and yolk sac were dissected, fixed in glutaraldehyde, and stained for 1acZ ovemight[12,17], then postfixed in 4% formalin, paraffin embedded and stained with haematoxylin-eosin.

TABLE 1 Morphometric analysis of blood-vessel development in 9.5-d.p.c. F_1 *VEGF*$^{+/+}$ and F_1 *VEGF*$^{+/-}$ embryos

	F_1 *VEGF*$^{+/+}$	F_1 *VEGF*$^{+/-}$
(*a*) Embryo		
Endothelial cells in the dorsal aorta		
Anterior	14 ± 0.7 (5)	5.0 ± 0.6 (5)‖***
Posterior	12 ± 1.5 (4)	8.0 ± 1.0 (7)
(*b*) Yolk sac		
Sections with large collecting vessels	73/104 (74%)	0/54 (0%)‡***
Size of small vessels (μm)†	90 ± 10	150 ± 20§***
Ratio of the cross-sectional vessel/yolk sac length (vessel density)†	0.82 ± 0.01	0.62 ± 0.07‖*
Number of endoderm cells surrounding a small vessel†	8.4 ± 0.5	15.9 ± 2.8‖*
Number of endothelial cells lining the endodermal side of a small vessel†	1.2 ± 0.2	2.7 ± 0.4‖*
Ratio of endothelial/endoderm cells per small vessel (endothelial cell density)†	0.15 ± 0.02	0.17 ± 0.02‖
BrdU-immunoreactive endothelial cells lining the endodermal side of a small vessel	159/428 (37%)	144/398 (36%)‡

(*a*) The data represent the mean ± s.e.m. of the number of endothelial cells lining the dorsal aorta (3–5 cross-sections per embryo), with the number of embryos indicated in parentheses. (*b*) The percentage of sections containing at least one large collecting yolk-sac vessel (arrow in Fig. 3*h*) was determined in four yolk sacs. The size (mean ± s.e.m.) of the small yolk-sac vessels is defined as the cross-sectional length, adjacent and parallel to the endoderm layer (c in Fig. 3*g*). Vessel density was defined as the ratio of the sum of the total cross-sectional vessel length, adjacent to the endodermal layer (c in Fig. 3*g*) versus total yolk-sac length (t in Fig. 3*g*) analysed (mean ± s.e.m.). For the number of endoderm cells (mean ± s.e.m.) surrounding a small vessel, see arrow in Fig. 3*g*. For the number of endothelial cells (mean ± s.e.m.) lining the endodermal side of the vessel, see arrowhead in Fig. 3*g*. Endothelial cell density was defined as the ratio of endothelial versus endoderm cells per vessel (mean ± s.e.m.). Cell counts represent the number of nuclear profiles. 5′-Bromo-2′-deoxyuridine (BrdU) labelling of cells was done by incubating yolk sacs in medium containing 30 μM BrdU for 60 min at 37 °C, followed by fixation in 4% formalin. BrdU immunostaining was performed using a biotinylated rat anti-BrdU antibody (clone BU1/75; Sera Lab, Sussex, UK) in an indirect immunostaining procedure, as previoiusly described[25].

† Measurements were taken using 80 yolk-sac vessels in four different yolk sacs.
‡ Statistical analysis used χ^2 tests.
§ Statistical analysis used Mann-Whitney test.
‖ Statistical analysis used analysis of variance.
* $P < 0.05$; *** $P < 0.001$ versus F_1 *VEGF*$^{+/-}$.

The formation of the extraembryonic vasculature in 9.5-d.p.c. F_1 VEGF$^{+/-}$ embryos was also defective. In addition to a dense plexus of small vessels, larger collecting vessels that connect with the embryo were observed in the yolk sac of 9.5d.p.c. F_1 VEGF$^{+/+}$ embryos (Fig. 3e, h). In contrast, the yolk sac of F_1 VEGF$^{+/-}$ embryos displayed an irregular plexus of small vessels but no larger collecting vessels (Fig. 3f, i). These results were confirmed by whole-mount staining with PECAM-specific antibodies of the yolk-sac vasculature (not shown) and by quantitative morphometric analysis, indicating the absence of such large collecting vessels in F_1 VEGF$^{+/-}$ yolk sacs (Table 1b). Morphometric analysis further showed that the diameter of the small vessels was enlarged but that fewer small vessels were present in F_1 VEGF$^{+/-}$ yolk sacs compared to those in F_1 VEGF$^{+/+}$ yolk sacs. The endothelial cell density and proliferation rate were, however, similar in both genotypes (Table lb). This may indicate that VEGF deficiency in the yolk sac affects normal fusion of angioblasts and the spatial organization of endothelial cells.

This study demonstrates that VEGF deficiency impaired most steps of early vascular development[23], including in situ differentiation of blood islands (vasculogenesis), sprouting from pre-existing vessels (angiogenesis), lumen formation, the formation of large vessels, the establishment of interconnections, and the spatial organization of intra- and extraembryonic vessels. Several factors may have contributed to this phenotype, including abnormal accumulation or delayed differentiation of endothelial cells (by VEGF acting as an endothelial cell-specific growth factor[2-5]), irregular fusion of angioblasts, and network formation of endothelial cells (possibly by VEGF acting in mediating cell-cell or cell-matrix contacts or in providing positional information), or by accelerated regression of pre-existing vessels (by VEGF acting as a survival factor for newly formed vessels', or owing to deficient or incorrect blood flow).

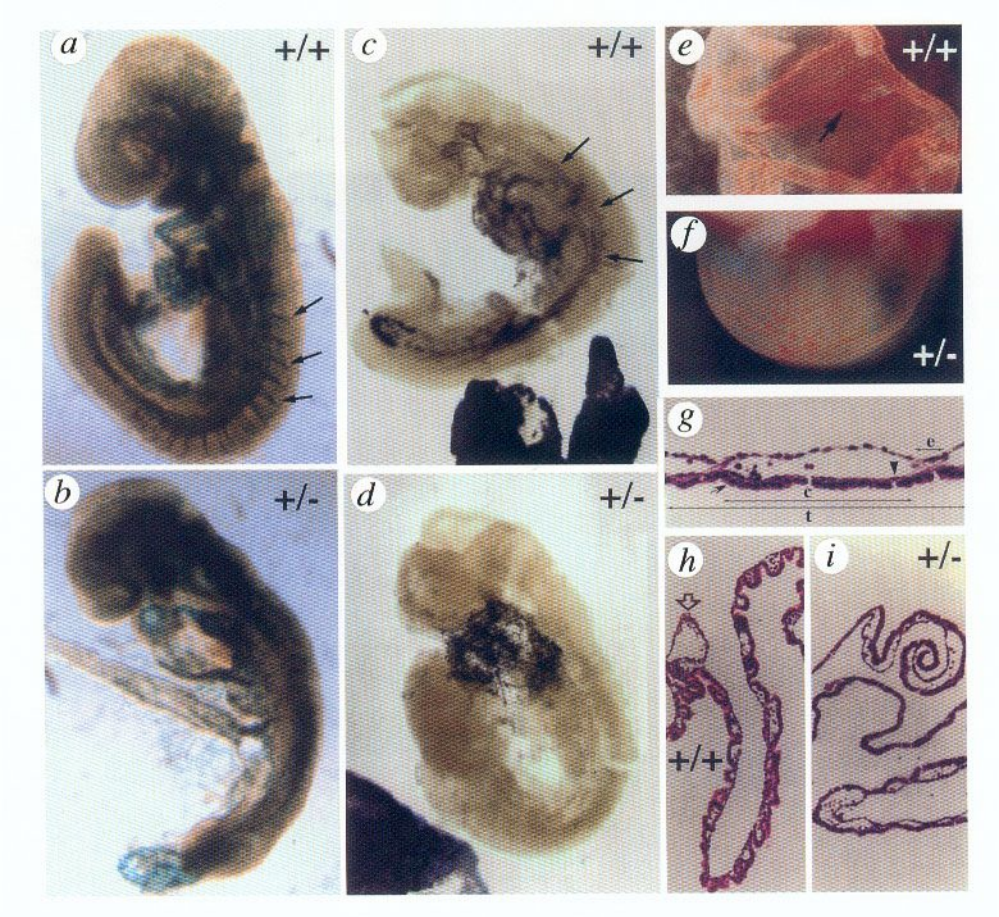

FIG. 3 a, b, Whole-mount LacZ staining revealing a dense network of sprouting vessels in the head mesenchyme and between the somites (arrows indicate intersomitic vessels), and the proper connections between the dorsal aortae and the heart of a 9.5-d.p.c. F_1 VEGF$^{+/+}$:tie-l-lacZ$^{+/-}$ embryo (a). The 9.5-d.p.c. F_1 VEGF$^{+/-}$: tie-1-lacZ$^{+/-}$ embryo (b) contained a dorsal aorta that appeared as a vascular string with a reduced diameter, fewer intersomitic vessels, and abnormal organization of vessels, connecting with the heart. c, d, Injection of ink made visible the heart and the major intra-embryonic vessels (including the dorsal aorta; arrows in c) in the riVEGF$^{+/+}$, but only the heart in the VEGF$^{+/-}$ T-ES cell-derived embryo (both at 9.5-d.p.c.). e, f, Macroscopic examination of the yolk sac revealing the presence of a dense capillary plexus with larger collecting vessels (indicated by arrow) in the 9.5-d.p.c. F, VEGF$^{+/+}$ yolk sac (e), but only an irregular and less dense network of wider capillaries without larger collecting vessels in the 9.5-d.p.c. F_1 VEGF$^{+/-}$ yolk sac fl. g, Section through a yolk sac, revealing an individual yolk-sac vessel with endothelial cells (arrowhead), and the visceral endoderm layer (arrow). Lines denote the cross-sectional length of the yolk-sac vessel, adjacent and parallel to the endoderm layer (c), the empty space between vessels (e) and the total yolk-sac length analysed (t). Measurements of these distances were used to calculate the vessel density (see Table 1b). h,i, Sections through a 9.5-d.p.c. F_1 VEGF$^{+/+}$ yolk sac (h), revealing a network of small vessels and a larger collecting vessel (open arrow), that connects with the intra-embryonic vitelline vessel. Sections through a 9.5-d.p.c. F_1 VEGF$^{+/-}$ yolk sac (i) revealed fewer but enlarged small yolk-sac vessels, and the absence of the larger collecting vessels.

METHODS. T-ES-derived embryos were dissected at 9.5-d.p.c. and filtered ink was immediately injected into the beating heart, using a heat-drawn capillary and a Narashigi micro-syringe-based injector. Dissection, fixation and staining of the embryos were done as described in Fig. 2.

Several novel findings have emerged from this study. (1) The delayed endothelial cell differentiation in VEGF deficiency is different from the aborted endothelial cell development in Flk-1 deficiency[12], suggesting either the existence of other (unknown) Flk-1 ligand(s), or the rescue of the Flk-l-related defect by maternal VEGF. This is unlikely, however, because of its paracrine mode of action[10,11] and the abnormal vascular development inside $VEGF^{+/-}$ or $VEGF^{-/-}$ T-ES-cell-derived embryos, despite the presence in the yolk sac of wild-type (tetraploid) endoderm cells[16,17] that produce VEGF[10,11]. (2) Heterozygous VEGF deficiency constitutes perhaps the most severe haploid-insufficient (autosomal) phenotype reported to date, which does not appear to be caused by imprinting of the residual wild-type allele (because of the significant expression of VEGF in $VEGF^{+/-}$ embryos), nor by interference with a dominant-negative VEGF mutant peptide (see Supplementary Information). This implicates a ligand dose-dependent effect of VEGF during vascular development, and the production of minimally required levels of VEGF during embryonic development in a highly regulated manner. (3) The similarity between phenotypes of embryos generated by aggregation of heterozygous mutant ES cells with tetraploid hosts, and embryos obtained by germline transmission, demonstrates the validity of this method to determine the phenotype of genetically altered embryos. This technology is fast and relatively inexpensive (as it does not require animal breeding), and separates extraembryonic and embryonic phenotypes by providing wild-type extraembryonic membranes to the mutant embryo[16,17]. It has also allowed to study the consequences of homozygous deficiency of a gene that is already embryonic lethal in heterozygous-deficient embryos.

Received 30 November 1995; accepted 29 January 1996.

1. Klagsbrun, M. & Solker, S. Curr. Biol. 3, 699-702 (1993).
2. Dvorak, H. F., Brown, L. F., Detmar, M. & Dvorak, A. M. Am. J. Path. 146, 1029-1039 (1995).
3. Plate, K. H., Breier, G. & Risau, W. Brain Path. 4, 207-218 (1994).
4. Neufeld, G., Tessler, S., Gitay-Goren, H., Cohen, T. & Levi, B-Z. Prog. Growth Factor Res. 5, 89-97(1994).
5. Ferrara, N. Trends Cardiovasc. Med. 3, 244-250 (1993).
6. Shibuya, M. et al. Oncogene 5, 519-524 (1990).
7. Devries, C. et al. Science 255, 989-991 (1992).
8. Millauer, B. et al. Cell 72, 835-846 (1993).
9. Mustonen, T. & Alitalo, K. J. Cell Biol. 129, 895-898 (1995).
10. Breier, G., Albrecht, U., Sterrer, S. & Risau, W. Development 114, 521-532 (1992).
11. Breier, G., Clauss, M. & Risau, W. Dev. Dynam. 204, 228-239 (1995).
12. Shalaby, F. et al. Nature 376, 62-66 (1995).
13. Fong, G.-H., Rossant, J., Gertsenstein, M. & Breitman, M. L. Nature 376, 66-70 (1995).
14. Maglione, D., Guernero, V., Viglietto, G., Delli-Bovi, P. & Parsee, M. G. Proc. Natl. Acad. Sci. U.S.A. 88, 9276-9271 (1991).
15. Park, J. E., Chen, H. H., Winer, J., Houck, K. A. & Ferrara, N. J. biol. Chem. 269, 25646-25654 (1994).
16. Nagy, A., Rossant, J., Nagy, R., Abramow-Newerly, W. & Roder, J. C. Proc. Natl. Acad. Sci. U.S.A. 90,8424-8428(1993).
17. Nagy, A. & Rossant, J. in Gene targeting. A Practical Approach (ed. Joyner, A. L.) 147-180 (IRL, Oxford, 1994).

18. Tischer, E. at al. J. Biol. Chem. 266, 11947-11954 (1991).
19. Claffey, K. P., Sanger, D. R. & Spiegelman, B. M. Biochim. Biophys. Acta 1246, 1-9 (1995).
20. Pötgen, A. J. G. et al. J. biol. Chem. 269, 32879-32885 (1994).
21. Friedrich, G. & Soriano, P. Genes Dev. 5, 1513-1523 (1991).
22. Puri, M., Rossant, J., Alitalo, K., Bernstein, A. & Partanen, J. EMBOJ. 14, 5884-5891 (1995).
23. Risau, W. & Flamme, I. A. Rev. Cell. Dev. Biol. 11, 73-92 (1995).
24. Alon, T. at al. Nature Med. 1, 1024-1028 (1995).
25. Tybulewicz, V. et al. Cell 65, 1153-1163 (1991).
26. Carmeliet, P. et al. J. Clin. Invest. 92, 2746-2755 (1993).
27. Risau, W. et al. Development 102, 471-478 (1988).
28. Stavri, G. T. et al. FEBS Lett. 358, 311-315 (1995).

SUPPLEMENTARY INFORMATION. Available at Nature's World-Wide Web site http://www.nature.con; requests may also be addressed to Mary Sheehan at the London editorial office of Nature.

ACKNOWLEDGEMENTS We thank K. Alitalo, A. Bernstein, J. Partanen, M. Puri and J. Rossant for the tie-l-lacZ transgenic mice; A. Damert for sequence information of the murine VEGF genomic clone; J. Herz for the JH, ES cells; and M. Baes, G. Carmeliet, M. Clauss, E. Conway, C. Lobe, M. Minne, J. Rossant and M. Sass and the other members of the CTTGT for help and discussions.

CORRESPONDENCE and requests for materials should be addressed to D. C. (e-mail: desire. collen@med.kuleuven.ac.be).